Electronic Supplementary Material (ESI) for Organic & Biomolecular Chemistry

Supplimentary information

An alternative approach: A highly selective dual responding fluoride sensor having active methylene group as binding site

Priyadip Das, Manoj K. Kesharwani, Amal K. Mandal, E. Suresh, Bishwajit Ganguly* and Amitava Das*

Central Salt and Marine Chemicals Research Institute (CSIR),
G.B. Marg, Bhavnagar: 364002, Gujarat, India.
Email address: ganguly@csmcri.org, amitava@csmcri.org
Telephone number: +91 278 2567760 [672]; Fax number: +91 278 2567562/6970

Table of Contents:-

^{1}H NMR spectra of L

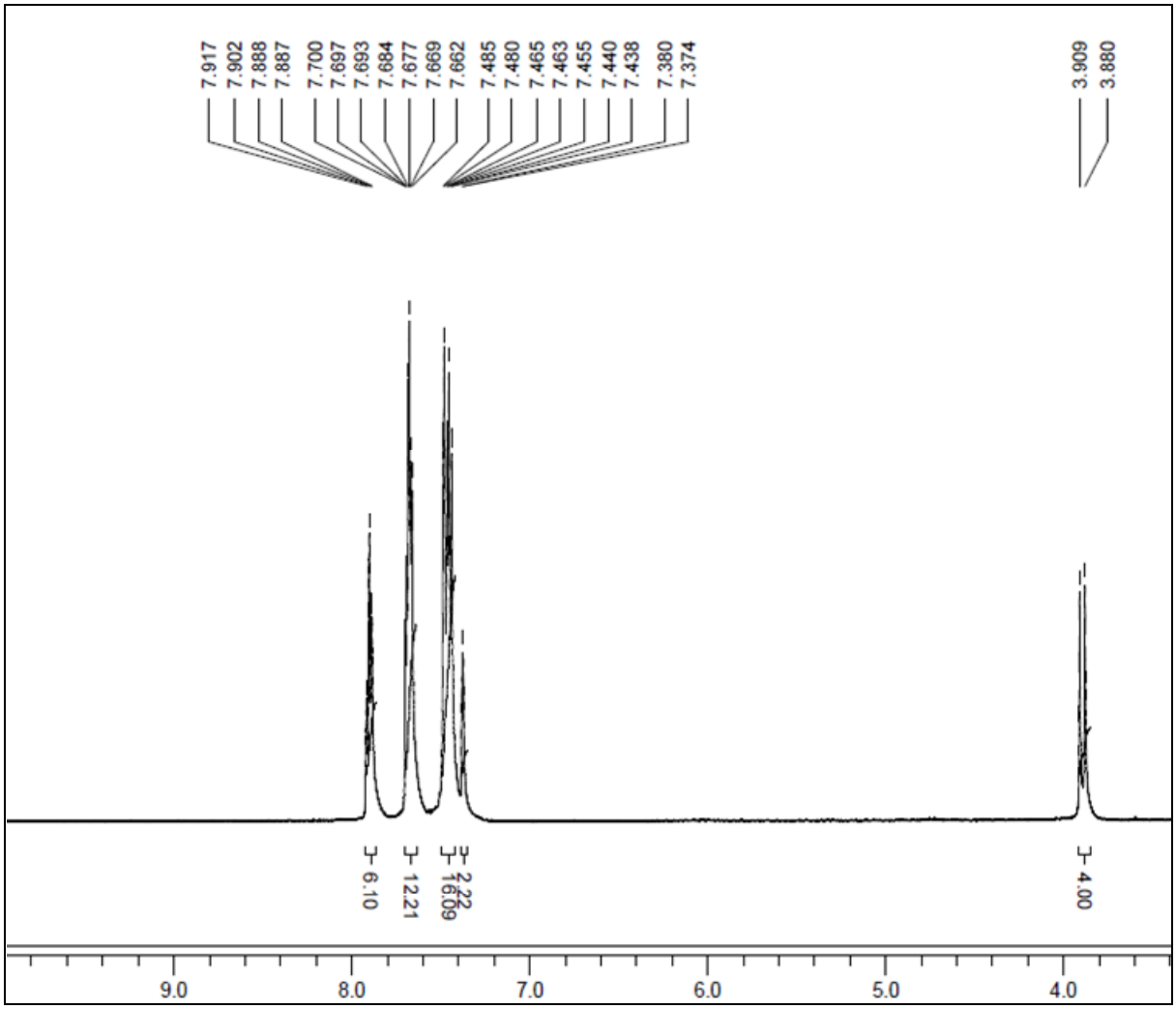

SI Figure 1:- ^{1}H NMR spectra of **L** in CD_3CN medium.

^{13}C NMR spectra of L

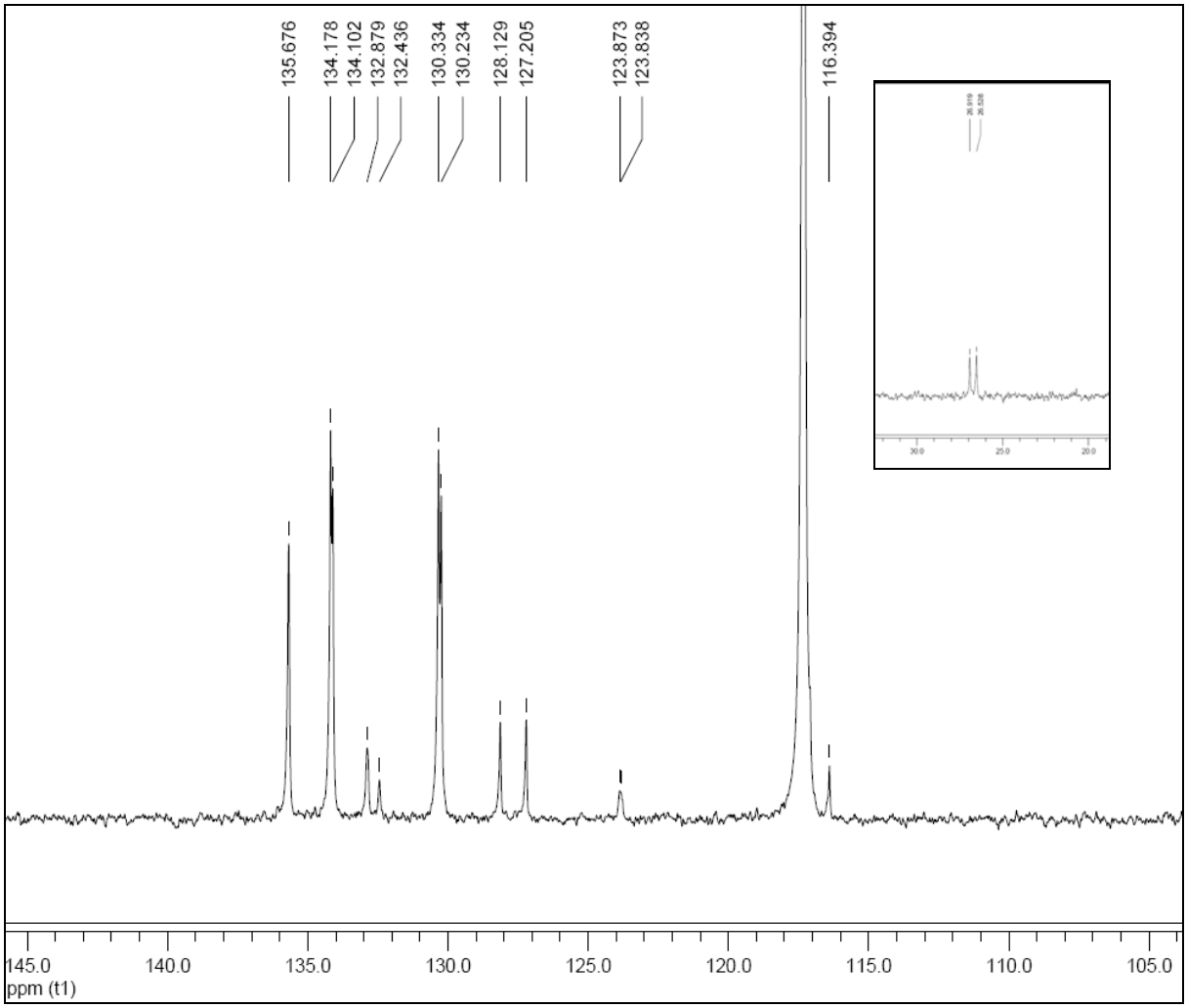

SI Figure 2:- ^{13}C NMR spectra of **L** CD_3CN medium.

IR spectra of L

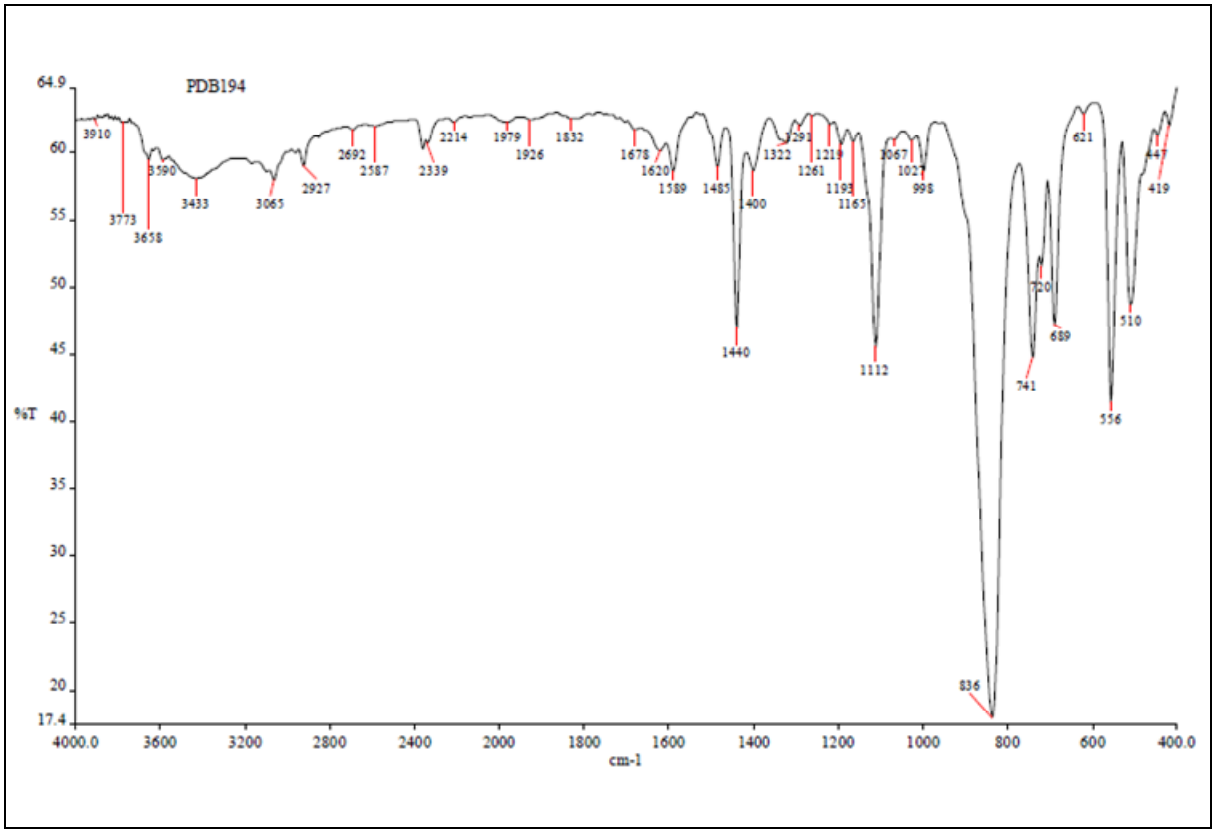

SI Figure 3:- FTIR spectra of **L** as KRB pellet.

ESI-MS spectra of L

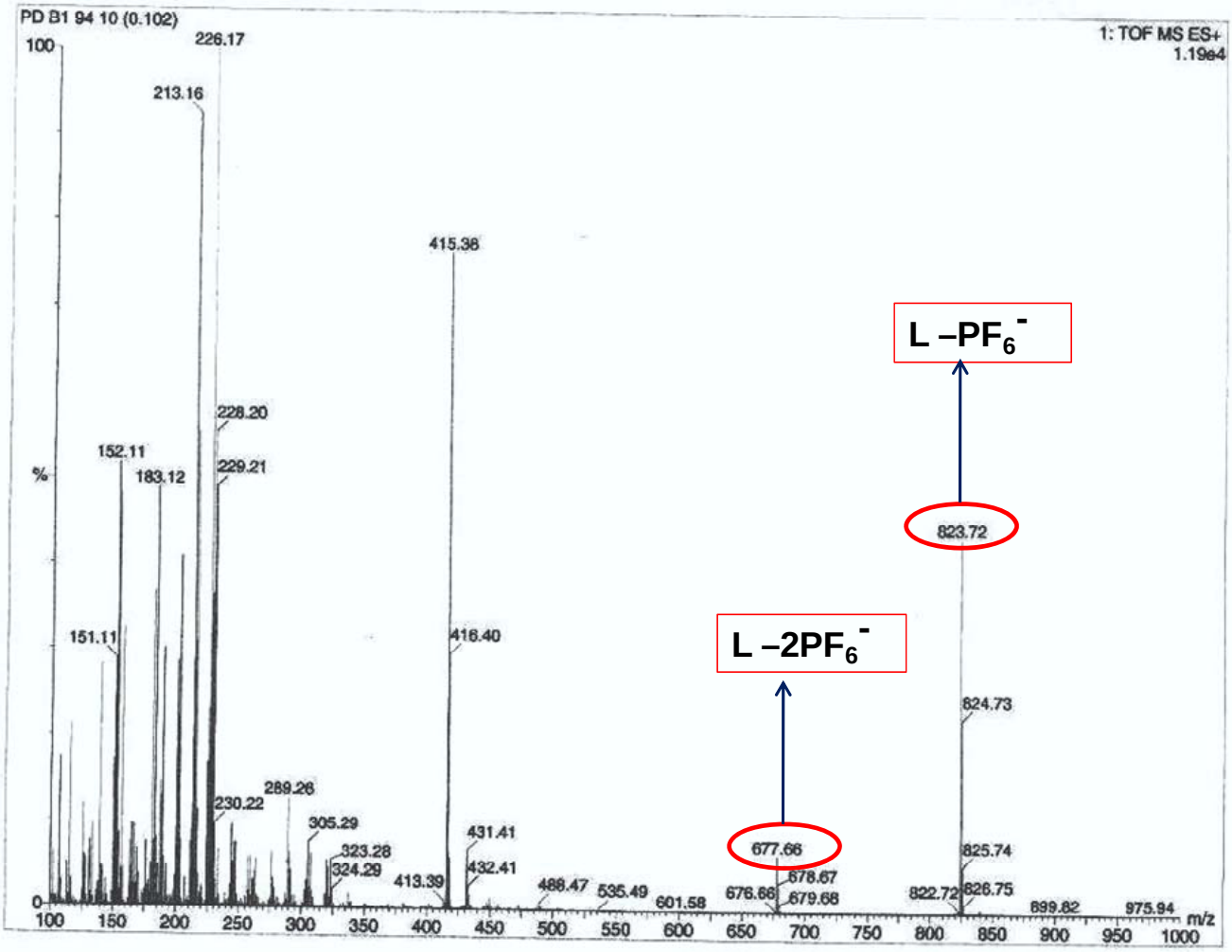

SI Figure 4: ESI-mass spectra of **L**.

UV response of L towards different Anions.

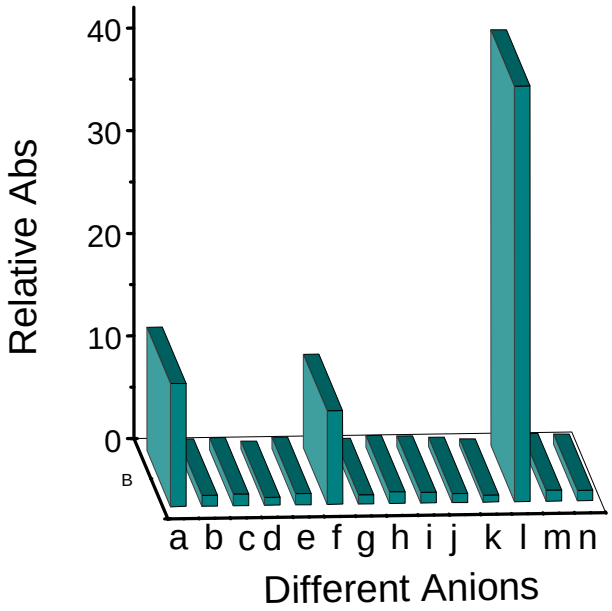

SI Figure 5: UV response of **L** (4.0 x10^{-5} M) in CH_3CN medium on addition of the solution of tetrabutyl ammonium salt of various anions(8.0 x 10^{-4} M) : a) CN^-, b) ClO_4^-, c) $PhCO_2^-$, d) IO_4^-, e)N_3^-, f) $H_2PO_4^-$, g) I^- , h) Br^- , i) $CH_3CO_2^-$, j) Cl^-, k) NO_3^-, l) F^-, m) HSO_4^-, n) L. with λ_{mon} = 358 nm.

Luminescence response of L towards different Anions.

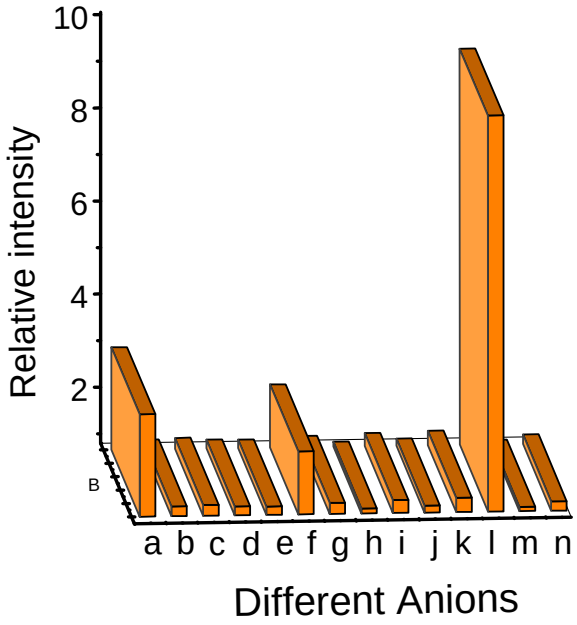

SI Figure 6: Luminescence response of **L** (2.0 x10^{-5} M) in CH_3CN medium on addition of the solution of tetrabutyl ammonium salt of various anions : (4.0 x10^{-4} M) : a) CN^-, b) ClO_4^-, c) $PhCO_2^-$, d) IO_4^-, e)N_3^-, f) $H_2PO_4^-$, g) I^- , h) Br^- , i) $CH_3CO_2^-$, j) Cl^-, k) NO_3^-, l) F^-, m) HSO_4^-, n) L with λ_{mon} = 366 nm and λ_{ext} = 280 nm.

UV- visible Titration of L with Fluoride

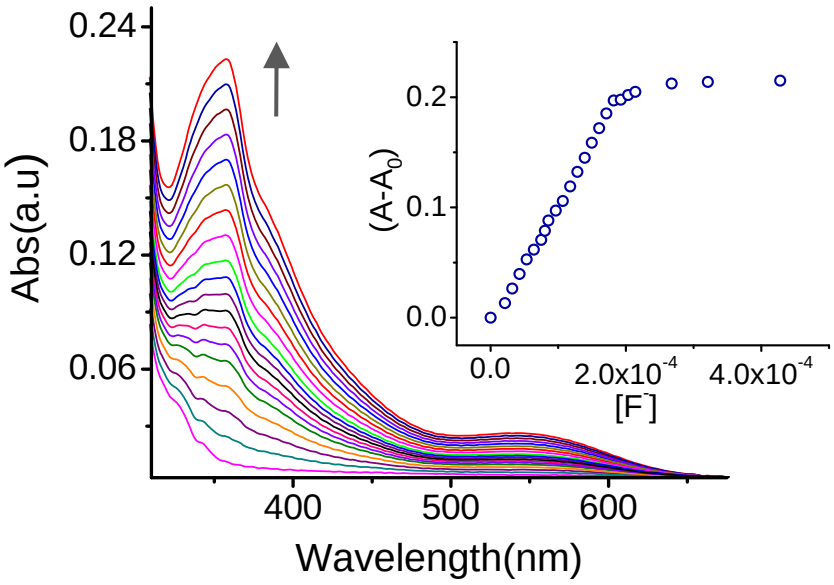

SI Figure 7: Absorption spectra of **L** (4.0×10^{-5} M) in presence of varying concentration of Fluoride [0 – 6.0×10^{-4} M] in acetonitrile medium. Inset: corresponding titration plot of **L** at 358 nm ($A-A_0$) as function of [F^-].

Benesi-Hildebrand plot of L with Fluoride (UV-Vis Titration)

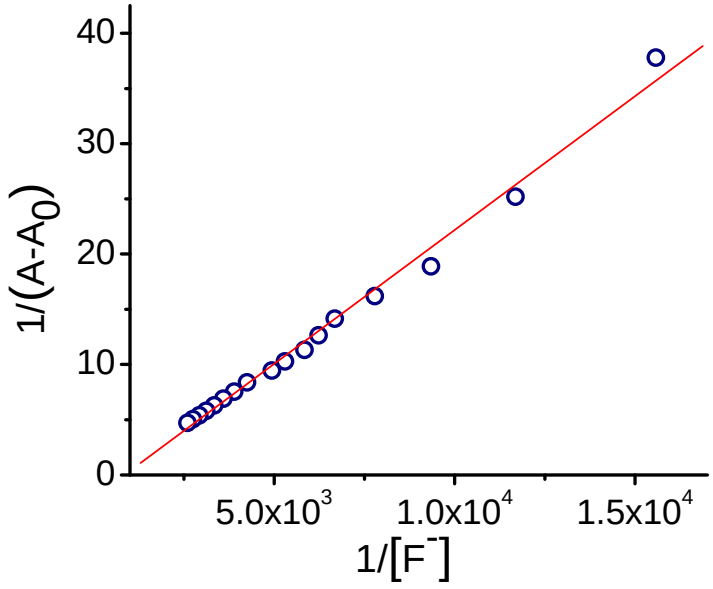

SI Figure 8: Benesi-Hildebrand plot of **L** with fluoride ion when monitoring absorbance changes at 358 nm. Good linear fit confirms the 1:1 binding stoichiometry.

Emission Titration of L with Fluoride

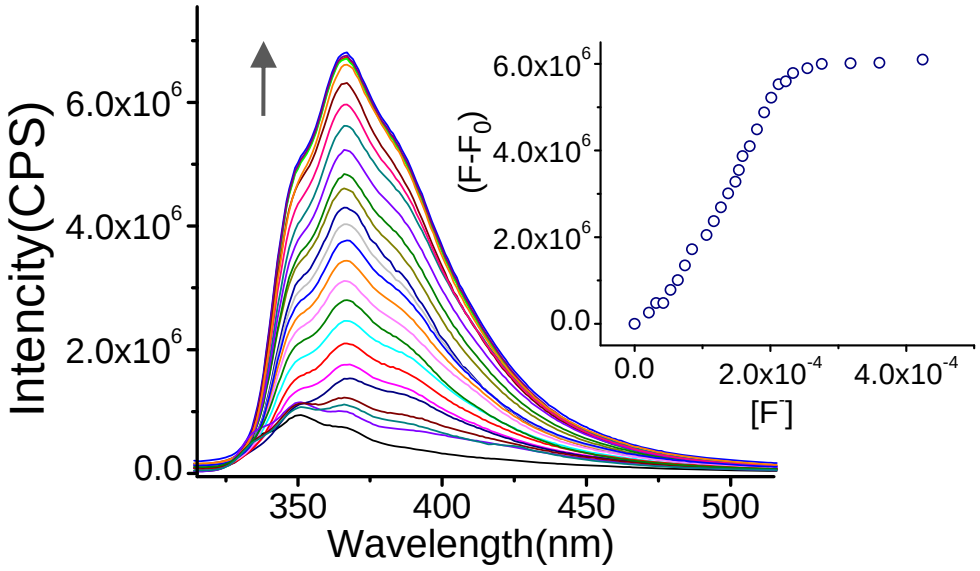

SI Figure 9: Emission spectra of **L** (2.0 x 10^{-5} M) in presence of varying concentration of Fluoride [0 – 3.15 x 10^{-4} M] in acetonitrile medium. Inset: corresponding titration plot of **L** at 366 nm ($F-F_0$) as function of [F^-].

Benesi-Hildebrand plot of L with Fluoride (Emission titration)

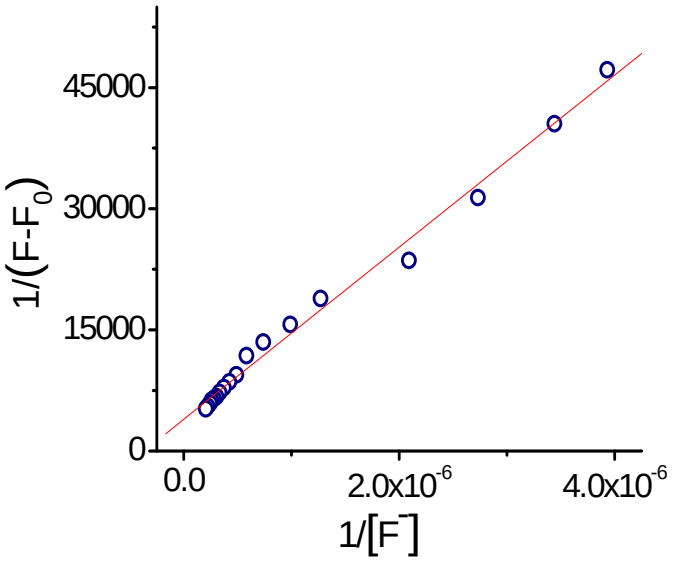

SI Figure 10: Benesi-Hildebrand plot of **L** with fluoride ion when monitoring emission intensity changes at 366 nm. Good linear fit confirms the 1:1 binding stoichiometry.

UV- visible Titration of L with di hydrogen phosphate

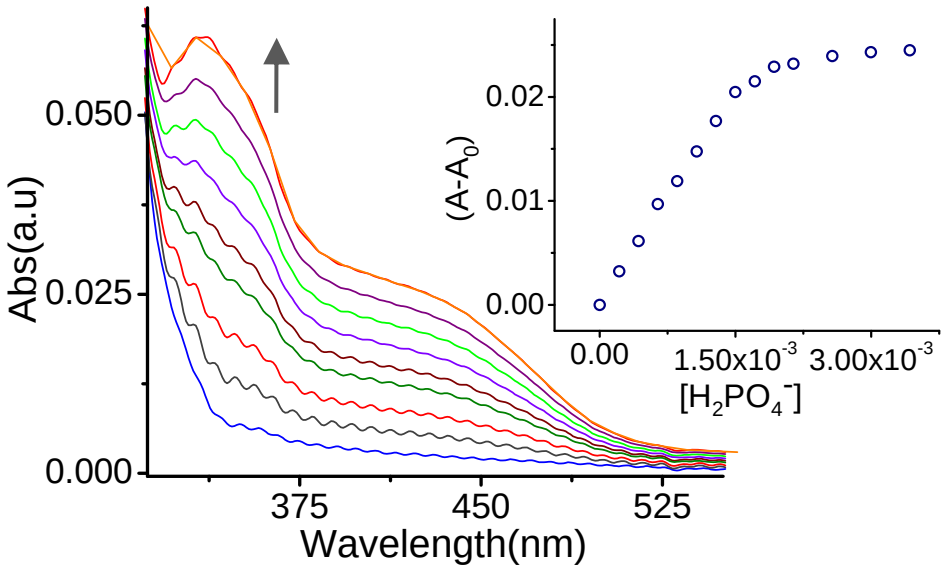

SI Figure 11: Absorption spectra of **L** (4.26×10^{-5} M) in presence of varying concentration of $H_2PO_4^-$ [0 – 1.72×10^{-3} M] in acetonitrile medium. Inset: corresponding titration plot of **L** at 420 nm ($A-A_0$) as function of [$H_2PO_4^-$].

Benesi-Hildebrand plot of L with $H_2PO_4^-$ (UV-Vis Titration)

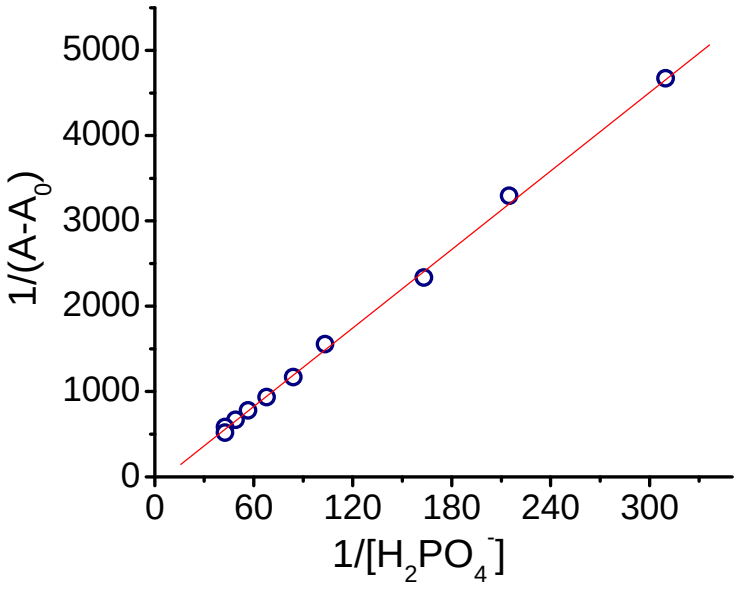

SI Figure 12: Benesi-Hildebrand plot of **L** with $H_2PO_4^-$ ion when monitoring absorbance changes at 420 nm. Good linear fit confirms the 1:1 binding stoichiometry.

Emission Titration of L with dihydrogen phosphate ion:

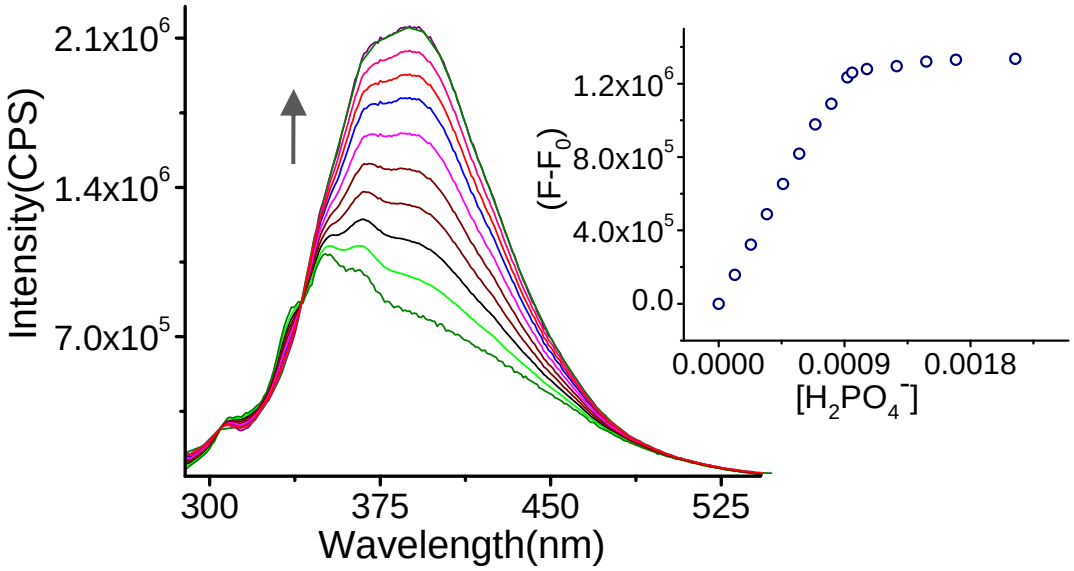

SI Figure 13: Emission spectra of **L** (2.10 X 10^{-5} M) in presence of varying concentration of $H_2PO_4^-$ [0 – 8.54 X 10^{-4} M] in acetonitrile medium. Inset: corresponding titration plot of **L** at 385 nm ($F-F_0$) as function of $[H_2PO_4^-]$.

Benesi-Hildebrand plot of L with $H_2PO_4^-$ (Emission titration)

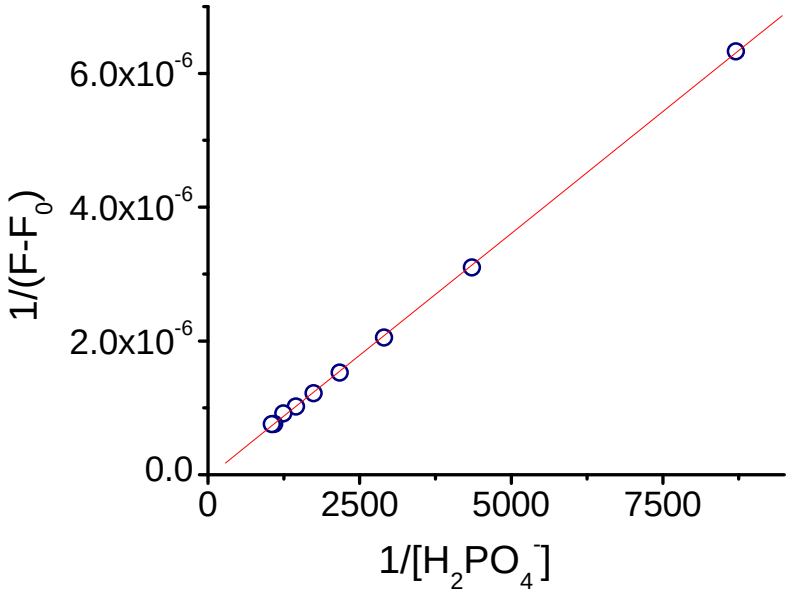

SI Figure 14: Benesi-Hildebrand plot of **L** with $H_2PO_4^-$ ion when monitoring emission intensity changes at 385 nm. Good linear fit confirms the 1:1 binding stoichiometry.

UV- visible Titration of L with CN^-:

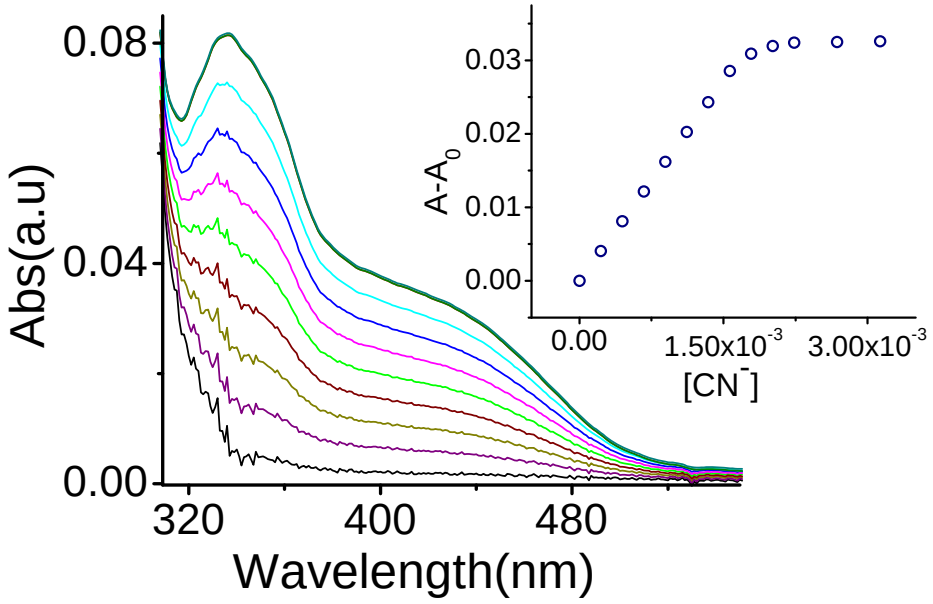

SI Figure 15: Absorption spectra of **L** (4.26×10^{-5} M) in presence of varying concentration of CN^- [0 – 1.78×10^{-3} M] in acetonitrile medium. Inset: corresponding titration plot of **L** at 420 nm ($A-A_0$) as function of [CN^-].

Benesi-Hildebrand plot of L with CN^- (UV-Vis Titration)

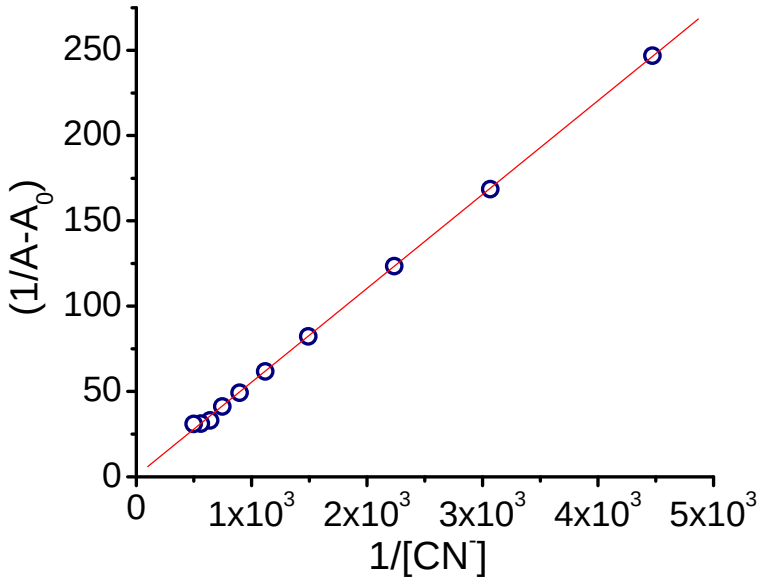

SI Figure 16: Benesi-Hildebrand plot of **L** with CN^- ion when monitoring absorbance changes at 420 nm. Good linear fit confirms the 1:1 binding stoichiometry.

Emission Titration of L with Cyanide

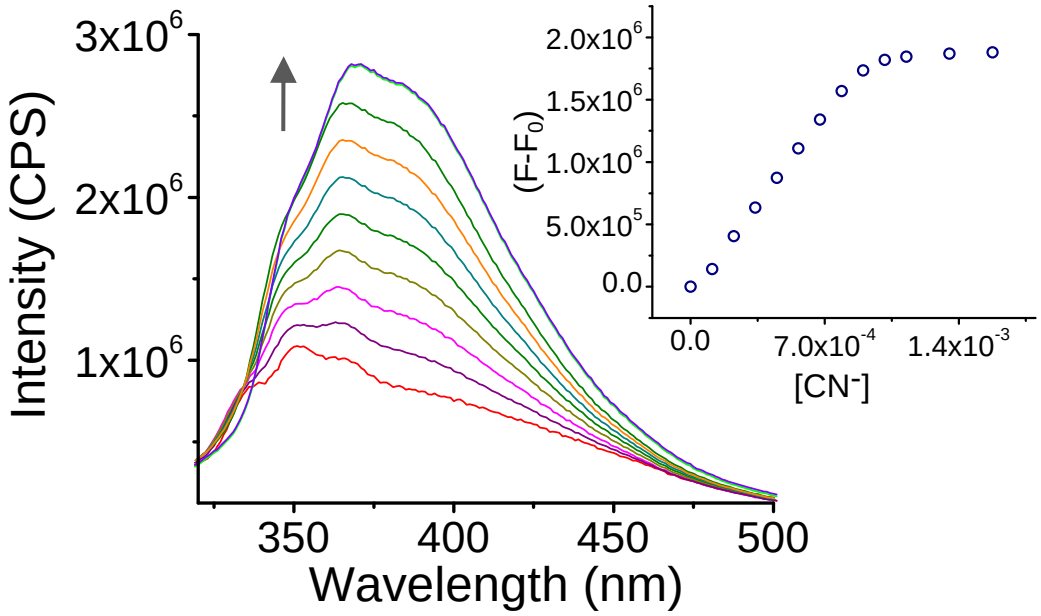

SI Figure 17: Emission spectra of **L** (2.10 X 10^{-5} M) in presence of varying concentration of CN^- [0 – 9.00 X 10^{-4} M] in acetonitrile medium. Inset: corresponding titration plot of **L** at 370 nm ($F-F_0$) as function of [CN^-].

Benesi-Hildebrand plot of L with CN^- (Emission titration)

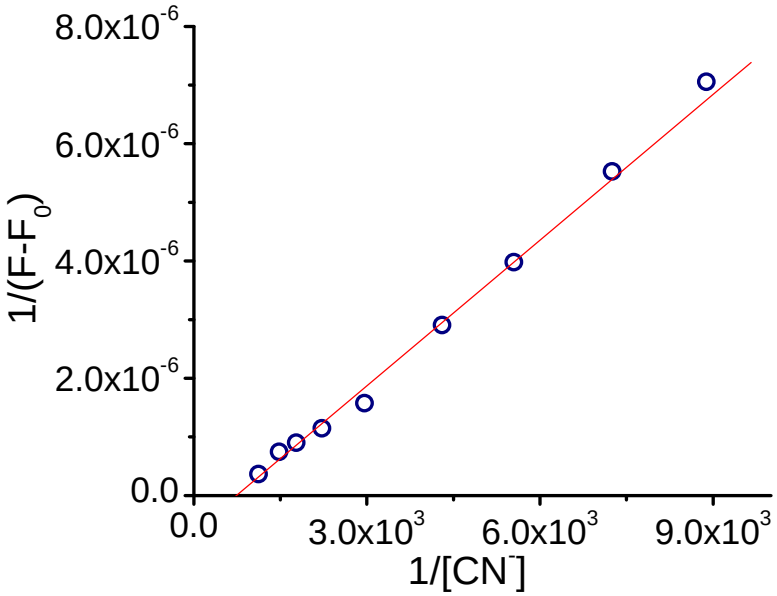

SI Figure 18: Benesi-Hildebrand plot of **L** with CN^- ion when monitoring emission intensity changes at 370 nm. Good linear fit confirms the 1:1 binding stoichiometry.

Mass spectra of (1:1) complex of Fluoride with L

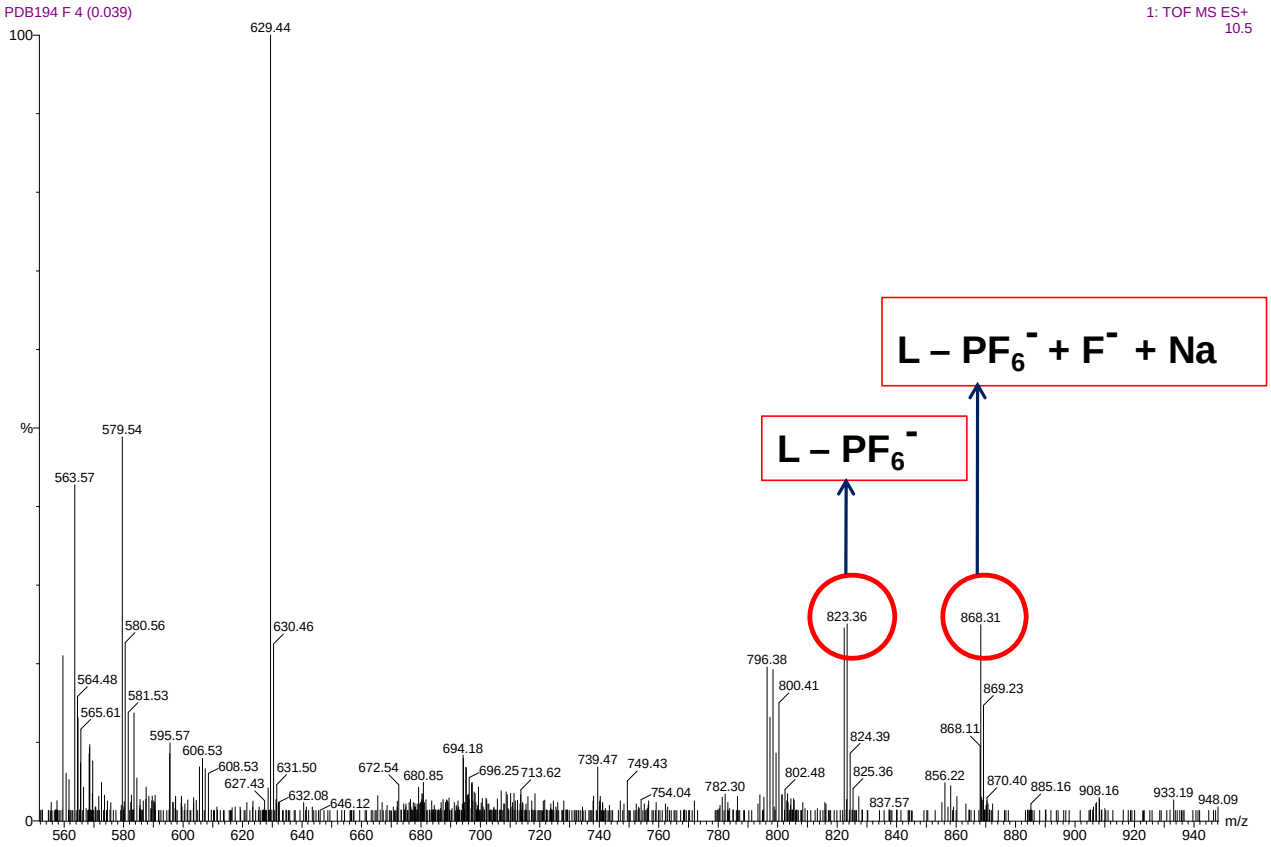

SI Figure 19: ESI-mass spectra of (1:1) complex of **L** and Fluoride.

Mass spectra of (1:1) complex of $H_2PO_4^-$ with L

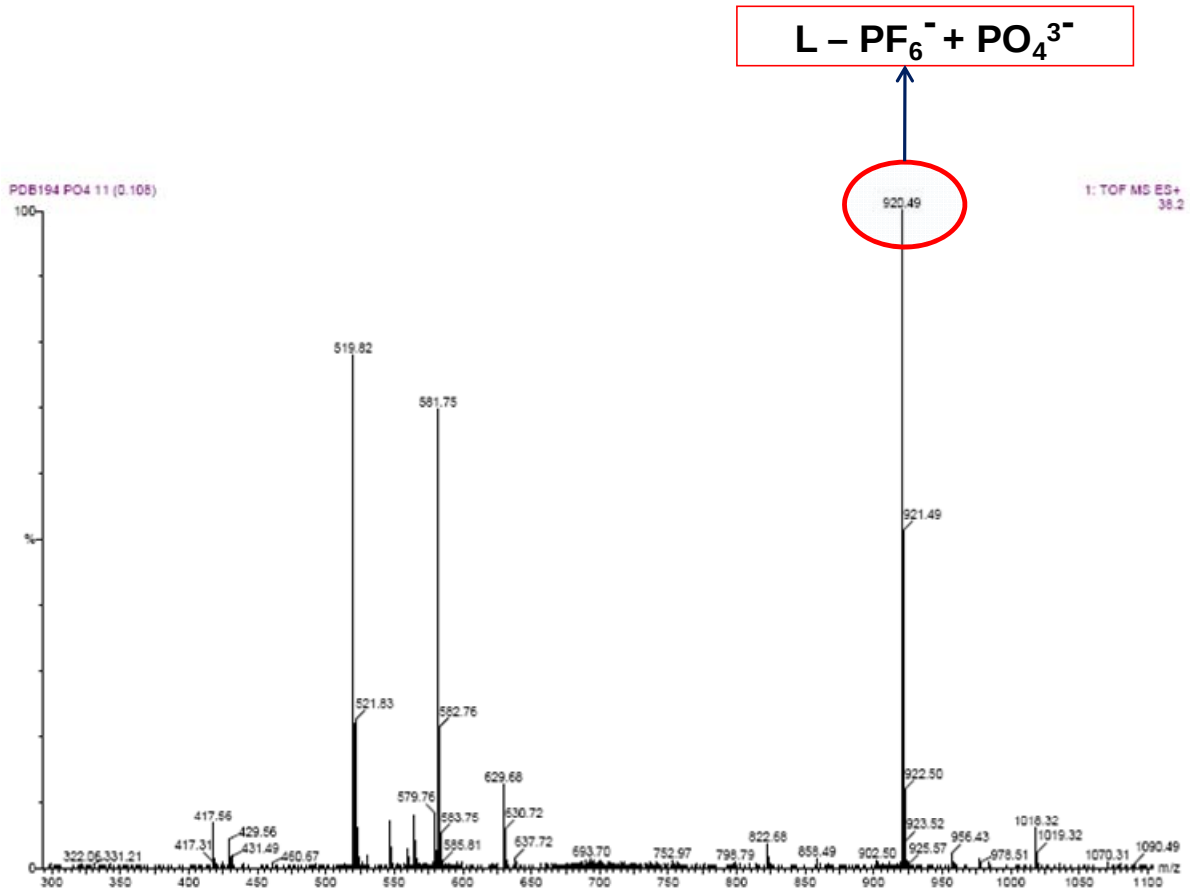

SI Figure 20: ESI-mass spectra of (1:1) complex of **L** and dihydrogen phosphate.

^{1}H NMR of L with different anions

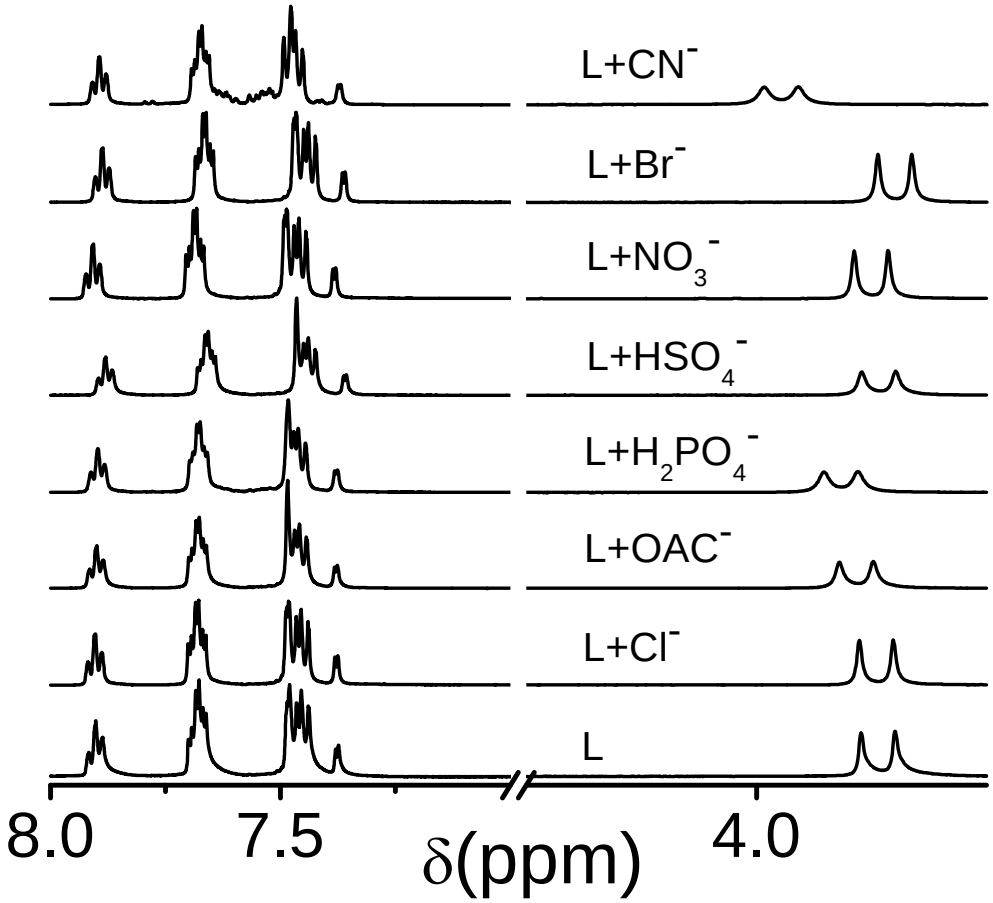

SI Figure 21: ^{1}H NMR spectra of compound **L** upon the addition of other different anions (30.00 equiv) in CD_3CN.

^{31}P NMR of L with different anions

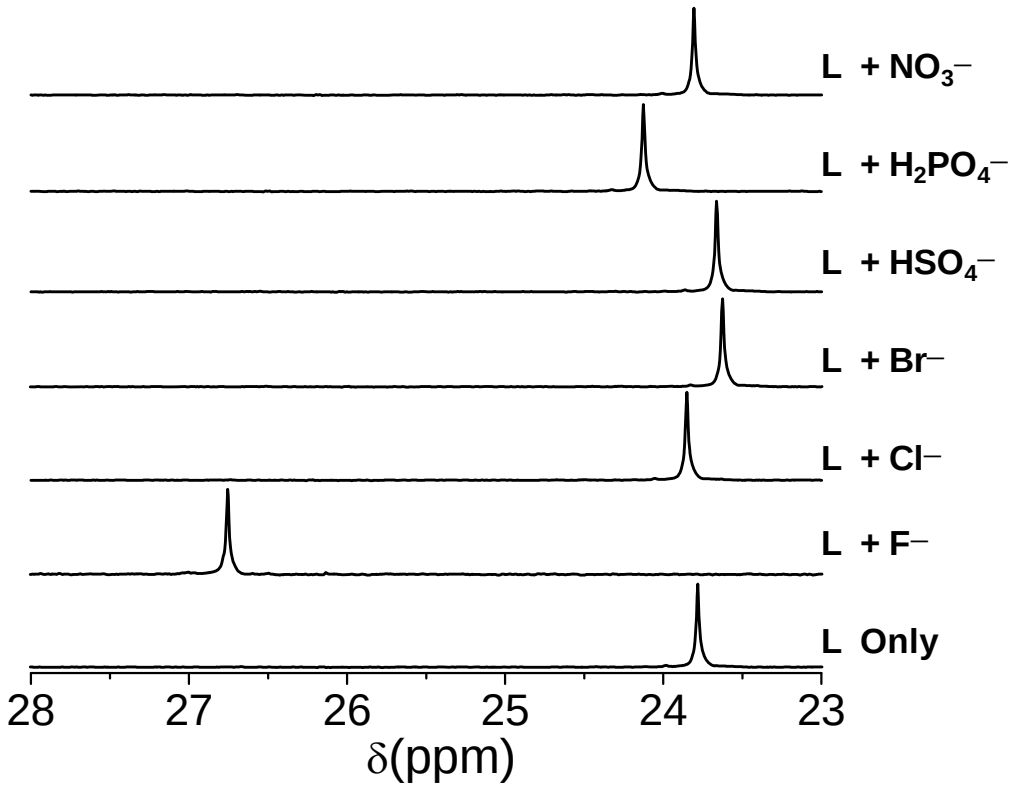

SI Figure 22: ^{31}P NMR spectra of compound **L** before and after addition of F^- (10equiv)and other anionic analytes $H_2PO_4^-$, Cl^-, Br^-, HSO_4^-, NO_3^- (30equiv) in CD_3CN at room temperature.

Excitation spectra for L.F$^-$ and L.CN$^-$ at emissive wavelength 366 nm

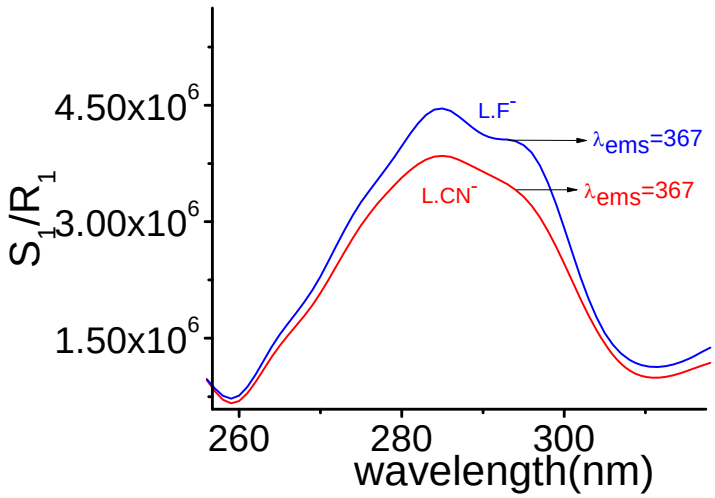

SI Figure 23: Excitation spectra recorded for **L.F$^-$** and **L.CN$^-$** at Emission wavelength 366nm

Job's plot analysis between L and TBA salts of F^-, CN^- and $H_2PO_4^-$

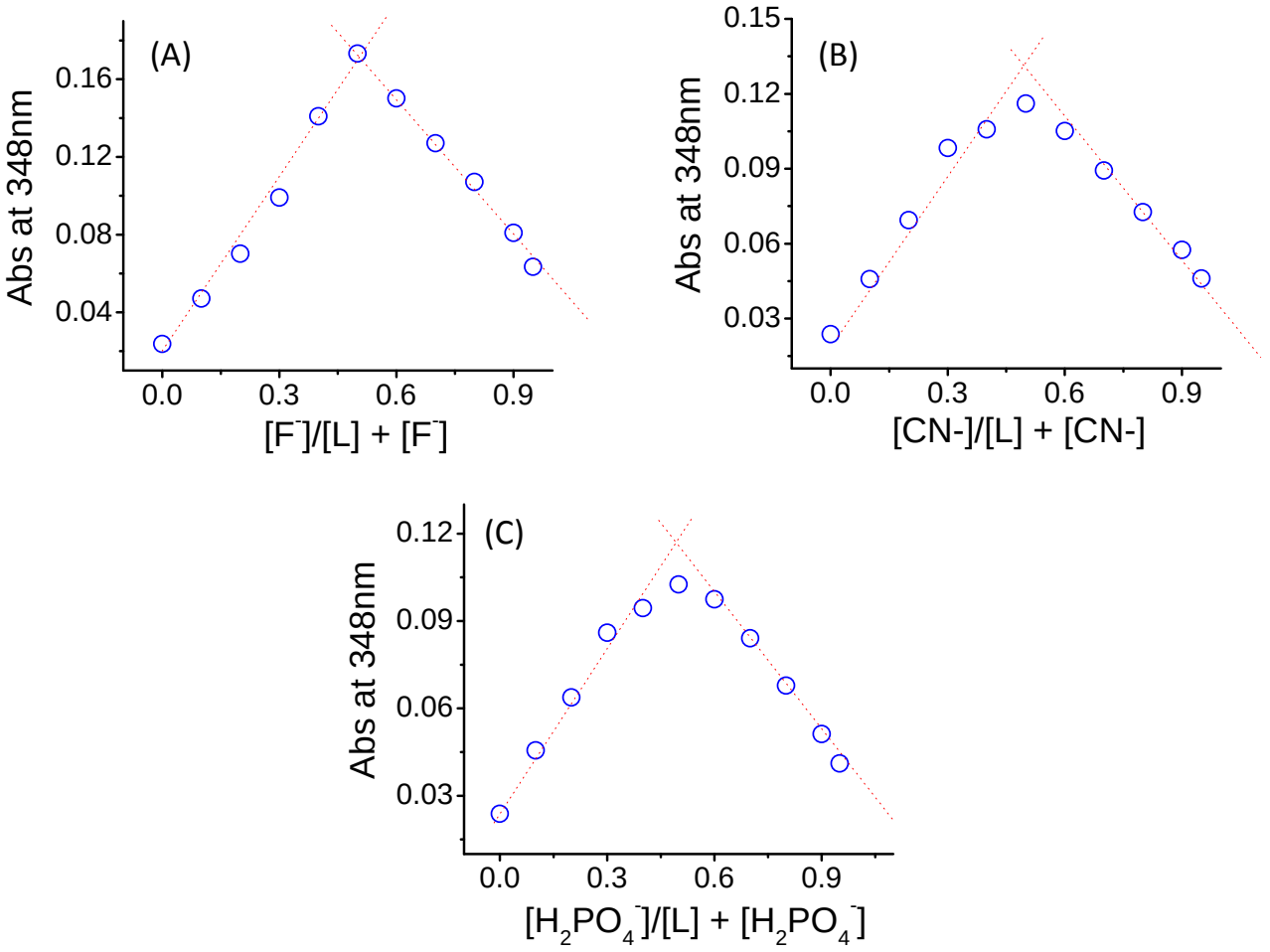

SI Figure 24: Job's plot analysis for the complexation between L and (A) F^-, (B) CN^- and (C) $H_2PO_4^-$. The total concentration of **L** and F^-/CN^- / $H_2PO_4^-$ were kept at 300 μM.

^{1}H NMR of L with different concentration of KO^{t}Bu

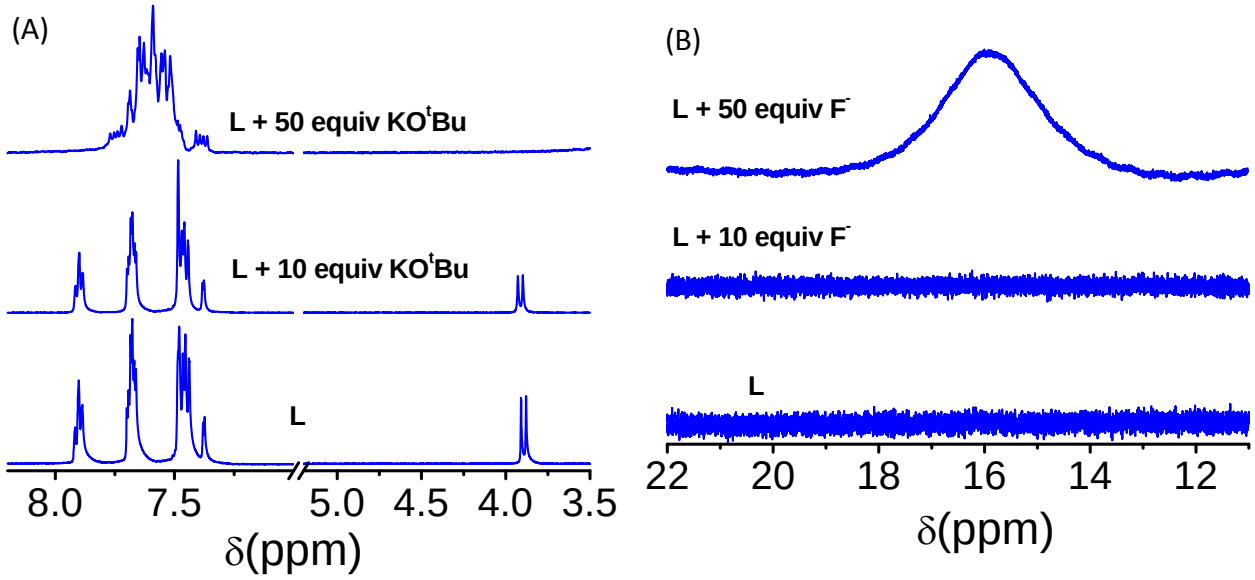

SI Figure 25: (A) ^{1}H NMR spectra of compound **L** upon the addition of varying concentration of KO^{t}Bu in DMSO (B) ^{1}H NMR spectra of **L** in absence and presence of varying concentration of F^- in DMSO(d_6) that reveals the generation of HF_2^- on deprotonation of L in presence of excess of F^- (50 mole equivalent). Deprotonation of L or the generation of HF_2^- was not evident with 10 mole equivalent of F^-

UV-VIS and emission scanning of L with Bu_4N-OH

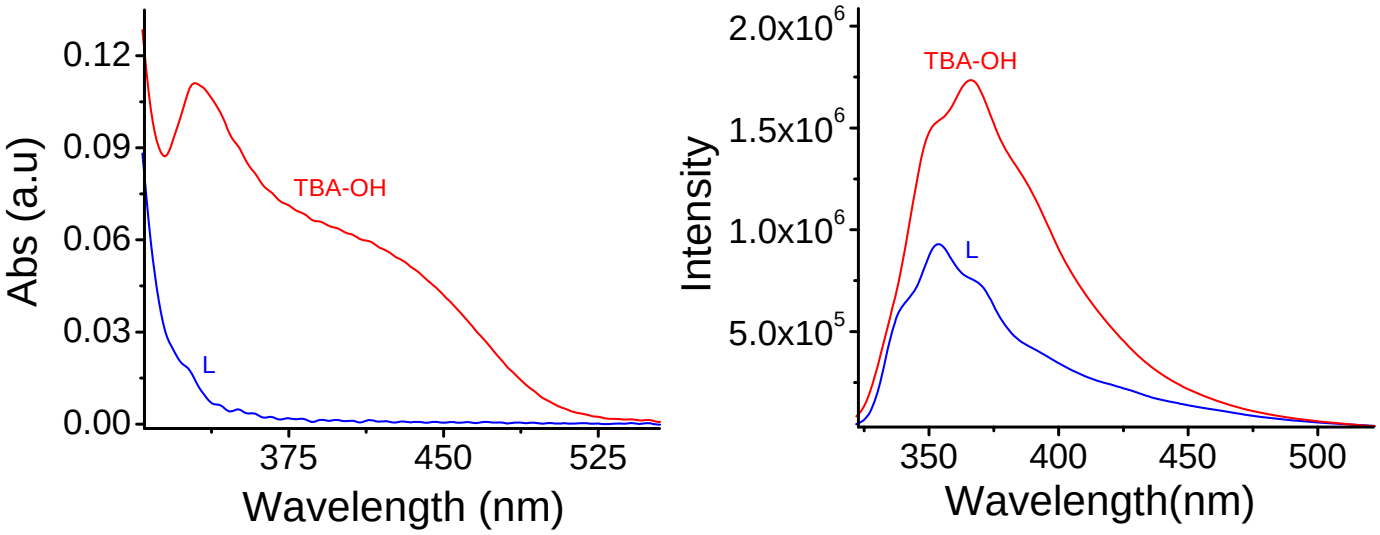

SI Figure 26: (A) Absorption spectra of L (4.0×10^{-5} M) in presence Bu_4NOH (10 mol Equivalent) (B) Emission spectra of L (2.0×10^{-5} M) in presence Bu_4NOH (10 mol Equivalent).